

# MPInterfaces: A Materials Project based Python Tool for High-Throughput Computational Screening of Interfacial Systems

Kiran Mathew<sup>a,c,\*</sup>, Arunima K. Singh<sup>b</sup>, Joshua J. Gabriel<sup>c</sup>, Kamal Choudhary<sup>c</sup>, Susan B. Sinnott<sup>d</sup>, Albert V. Davydov<sup>b</sup>, Francesca Tavazza<sup>b</sup>, Richard G. Hennig<sup>c,\*</sup>

<sup>a</sup>Department of Materials Science and Engineering, Cornell University, Ithaca, NY 14850, U.S.A.

<sup>b</sup>Materials Science and Engineering Division, National Institute of Standards and Technology, Gaithersburg, MD 20899, U.S.A.

<sup>c</sup>Materials Science and Engineering, University of Florida, Gainesville, FL 32611, U.S.A.

<sup>d</sup>Department of Materials Science and Engineering, The Pennsylvania State University, University Park, PA 16801, U.S.A

---

## Abstract

A Materials Project based open-source Python tool, *MPInterfaces*, has been developed to automate the high-throughput computational screening and study of interfacial systems. The framework encompasses creation and manipulation of interface structures for solid/solid hetero-structures, solid/implicit solvents systems, nanoparticle/ligands systems; and the creation of simple system-agnostic workflows for in depth computational analysis using density-functional theory or empirical energy models. The package leverages existing open-source high-throughput tools and extends their capabilities towards the understanding of interfacial systems. We describe the various algorithms and methods implemented in the package. Using several test cases, we demonstrate how the package enables high-throughput computational screening of advanced materials, directly contributing to the Materials Genome Initiative (MGI), which aims to accelerate the discovery, development, and deployment of new materials.

*Keywords:* Materials Genome Initiative, 2D Materials, Interfaces, Substrates, Heterostructures, Ligands, Nanocrystals, Wulff Construction, Workflows, Density-Functional Theory, MPInterfaces

---

## 1. Introduction

Interfaces play a vital role in practically all materials and devices [1, 2, 3, 4]. For instance, the efficiency and stability of electrochemical devices are mostly decided by the composition and the properties of the solid electrolyte interface layers [5]. In another example, the self assembly of nanoparticles used in high-efficiency photovoltaic devices is directed by the interfaces formed between nanoparticles, ligands and the solvent they are dispersed in [6, 7]. As materials and devices are getting smaller, the interface properties begin to dominate their essential characteristics. Progress in a wide variety of applications ranging from catalysis to microelectronics is guided by a refinement of our understanding and control of the interface properties.

Experimental studies combined with computational investigations provide a broad spectrum of information needed for an accurate and thorough understanding of interfaces, which is seldom accessible by utilizing one of these two approaches alone [8, 4, 9, 10, 11, 12]. Though combinatorial techniques are increasingly used by experimentalists for identifying new compositions as well as for the rapid optimization and mapping of processing parameters that influence the properties of materials, a complete experimental characterization of a large number of possible candidate systems poses a daunting challenge due to time-consuming and expensive experiments, besides limitations involved while exploring extreme and hazardous environmental conditions [13, 14, 15]. In order to complement and guide experimental investigations, and to accelerate the discovery of novel phenomenon at interfaces it is imperative to adopt a rational approach towards the screening and the char-

---

\*Corresponding author

Email addresses: km468@cornell.edu (Kiran Mathew), rhennig@ufl.edu (Richard G. Hennig)

acterization of interfacial systems. The advancement of modern computing has pushed the boundaries of materials simulations making them faster, more cost-effective, efficient and accurate. In recent years, high-throughput computational studies have predicted new materials for applications in photocatalysis, energy storage, piezoelectrics and electrocatalysis [16, 17, 18, 19, 20, 21, 22].

The study of materials interfaces presents additional challenges compared to bulk materials' properties due to the increased number of configurations and conformations possible in these two (or more) phase systems and requires larger computational resources due to the reduced symmetry of the system. To enable the high-throughput computational screening of the structure, stability, and properties of materials interfaces – such as between nanocrystals, ligands, and solvents and between 2D materials and substrates – we have developed the open-source Python package, *MPInterfaces*. First, the package automates the generation of various interfacial structures and prepares input files to first principles density-functional theory (DFT) simulations softwares like Vienna Ab-initio Software Package (VASP) [23] and molecular dynamics (MD) simulations softwares like Large-scale Atomic/Molecular Massively Parallel Simulator (LAMMPS) [24]. It then enables the creation of high-throughput computational workflows that can be deployed on remote computing resources. Finally, the package provides analysis tools such as for the prediction of the shape of nanocrystals using surface energies and the Wulff construction. The coupling with the energy calculation softwares and the workflow creation builds on the framework of the open source Python packages of the Materials Project namely pymatgen [25], custodian [25] and fireworks [26].

The package is being continuously developed and the latest version can be obtained from the GitHub repository at <https://github.com/henniggroup/MPInterfaces>. In the following sections we present an overview of the package using several examples, describe its capabilities, and discuss the algorithms we employed to overcome some of the technical and scientific challenges.

## 2. *MPInterfaces*: Overview with examples

The *MPInterfaces* package is written in Python 2.7 with support for Python 3.x. The package makes extensive use of existing Python tools for the generation and manipulation of various structures

and the creation of the corresponding input files for DFT and MD simulations. For the structural analysis and input file generation for the interfacial structures we extend the pymatgen package [25]. The Atomic Simulation Environment [27] package is used to interface with the MD software package LAMMPS. For the workflow creation and management we extend the custodian and the fireworks packages [25, 26]. In the following subsections we discuss the capabilities supported by the *MPInterfaces* package that are built on top of the aforementioned packages. Illustrative examples with corresponding code snippets are provided in each section to aid users in employing this framework.

### 2.1. *Ligand capped nanoparticles*

Nanocrystals in the form of quantum dots are increasingly employed in the fabrication of devices such as solar cells, transistors, and LEDs [28, 29]. Often the assembly of such nanocrystals into superlattices yields new materials with tunable optical and electronic properties [6, 7]. DFT calculations and MD simulations are routinely used to characterize interfaces properties that are hard to access with stand alone experiments, such as for example the binding energies and surface energy changes in varying environments of capping ligand and solvents [9, 7, 30].

It is well known that nanocrystal surface chemistry as well their shape evolution are controlled by the thermodynamics and kinetics of the three phase system comprising of the nanocrystals, surfactant molecules (also known as capping ligands) and the solvent [9]. Furthermore, the energetics of the system determines the thermodynamics and kinetic barriers of the growth of such nanocrystals, which drive their size, shape, and properties.

*MPInterfaces* enables a high-throughput computational screening of nanoparticle/ligand combinations by sampling the following degrees of freedom in the system: (a) the crystallographic planes of the surface facets, (b) the ligand binding sites on each facet, and (c) the ligand surface coverage for the given facet-ligand-binding site combinations. We model these interfaces using slab models of a specified thickness and crystallographic facet, and with ligands adsorbed on the surfaces. The construction of the slab model for an interface requires the specification of the following six parameters: (i) the bulk phase that constitutes the surface in question, (ii) the crystallographic facet of interest in this bulk phase, (iii) the initial binding site on the surface,

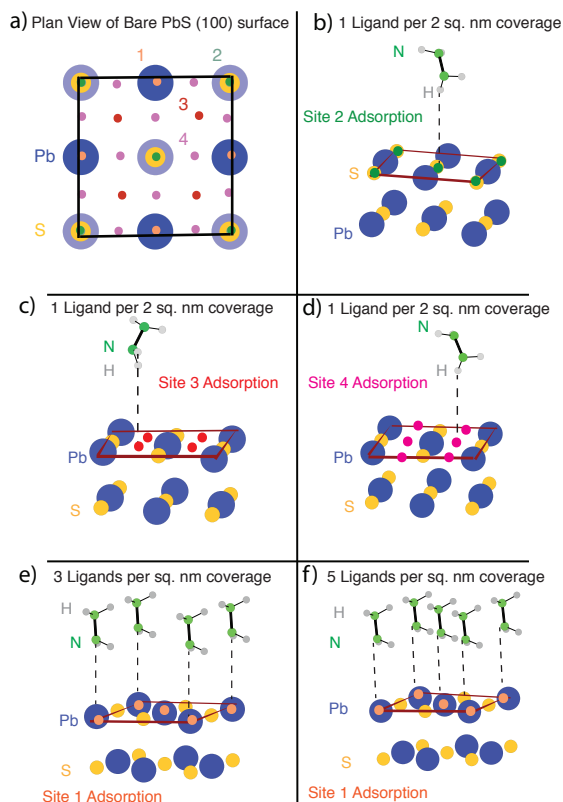


Figure 1: Specification of the structure of ligands adsorbed on PbS(100) facet. (a) Top view of a rocksalt PbS(100) facet with possible high-symmetry binding sites 1,2,3,4 marked as orange, green, purple and red circles, respectively. The Pb atoms are shown in blue and S in yellow. (b) A hydrazine ligand is placed on site 2, above a S atom bound through the H atom of the ligand, (c) site 3 of PbS(100) referenced with adsorption distance bound through the Hydrogen (H - Grey) atom on the ligand, (d) site 4 of PbS(100) bound through the N atom on the ligand with a random rotation about cartesian axes, (e) higher coverage on site 1 above a Pb atom, binding through N atom, (f) a high coverage over site 4, binding through N atom. Notice the preservation of symmetry between the molecules to minimize the steric hindrance. Other entropic configurations can be included with manual manipulation of binding sites.

(iv) the binding atom on the ligand that is intuitively expected to be the nearest neighbor to the chosen binding site on the surface, (v) the initial approximate separation between the surface binding site and the atom, which in other words is the adsorption distance, and (vi) the ligand coverage on the surface in number of ligands per unit area. Figure 1 illustrates as an example the degrees of freedom that can be controlled for an interface model of a (100) surface of PbS that is decorated with lead

acetate,  $\text{Pb}(\text{CH}_3\text{COO})_2$ , ligands.

The *interfaces.py* module in the package defines the Python classes for the creation of ligands from the combinations of different molecules. The molecule structures can be generated using the Python interface to openbabel [31] or directly read in from the locally available structure files of various formats supported by pymatgen. The ligands are then placed above a slab that is generated from a bulk structure by specifying the  $(hkl)$  Miller indices of the required facet. Figure 1 illustrates how the ligand configurations are specified through the binding sites and surface coverage. Additionally a liquid phase, such as a solvent or electrolyte, can be added to the nanoparticle-ligand interface in an efficient and accurate manner by using the implicit solvent or electrolyte models that are provided by the VASPsol module [32, 33].

The following code excerpt illustrates how the slab structure in Fig. 1(e) is generated in the *MP-Interfaces* framework.

```
# A code excerpt for generation of a single
# nanoparticle facet-ligand interface
# All distances are in Angstroms

from mpinterfaces.interface import Ligand, \
    Interface

Bulk_struct = Structure.from_file("POSCAR.
    bulk")
hkl = [1,0,0]
min_thick = 10
min_vac = 30
# ligands per sq. Angstroms
surface_coverage = 0.03
hydrazine = Molecule.from_file(
    "hydrazine.xyz")
ligand= Ligand([hydrazine])
# position the ligand
x_shift = 0.0
y_shift = 0.0
z_shift = 3.0
adsorb_on_species = 'Pb'
adatom_on_ligand='N'
interface = Interface(
    bulk_struct, hkl=hkl,
    min_thick=min_thick,
    min_vac=min_vac,
    ligand=ligand,
    displacement=z_shift,
    x_shift=x_shift, y_shift = y_shift
    adatom_on_lig=adatom_on_ligand,
    adsorb_on_species= adsorb_on_species,
```

```

        surface_coverage=surface_coverage)
interface.create_interface()

```

This code can be easily generalized to create and simulate arbitrary facets of bulk materials with atomic or molecular species adsorbed on the surface.

## 2.2. Wulff construction

As mentioned above, the shape of nanocrystals as well as their self-assembly into mesoscale structures depends strongly on the thermodynamics and kinetics of the system, comprised of the nanoparticles, ligands and solvent. The shape of a crystal or nanocrystal is given by the Wulff construction, which requires as input the surface energy of the crystal facets [34, 35, 36, 37].

For nanocrystal surfaces capped with ligands, the surface energy,  $\gamma_{hkl}$ , is a function of the ligand coverage and given by [7]

$$\gamma_{hkl} = \gamma_{hkl}^0 - \Theta_{hkl} E_{b,hkl},$$

where  $\gamma_{hkl}^0$  is the surface energy of the bare slab,  $\Theta_{hkl}$  is the surface coverage, and  $E_{b,hkl}$  is the binding energy of the ligand (positive values indicate strong binding). Given the surface energies of all facets of interest in the crystal structure, it is possible to predict the equilibrium shape of a nanocrystal, which is the multifaceted shape that minimizes the nanocrystal's surface energy. This shape can be obtained using the Wulff construction. Our implementation of the Wulff construction extends existing implementations for cubic symmetry to arbitrary space groups. The code takes advantage of the space group symmetry and utilizes the pymatgen symmetry tools to determine the symmetry-equivalent crystallographic facets.

The *nanoparticle.py* module in the *MPInterfaces* package implements the classes that let the user provide the list of Miller index families, their corresponding surface energies, and the maximum radius of the nanoparticle to create the equilibrium nanocrystal shape using the Wulff construction. The following code excerpt illustrates the construction of the equilibrium shape of the PbS nanocrystal shown in Figure 2. The surface energies of the three low-index (111), (100), and (110) facets of PbS in vacuum are taken from Ref. [32]. The surface energy of the (111) facet is for the reconstructed surface [7], however, we do not show the (111) surface

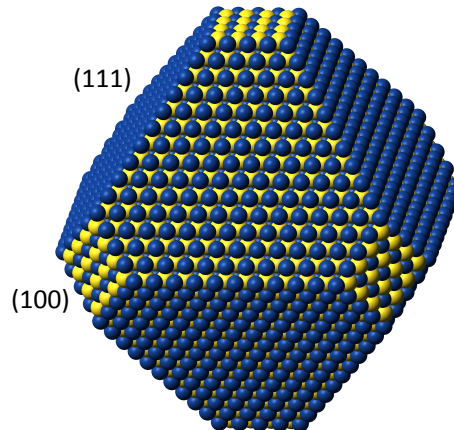


Figure 2: The shape of a PbS nanocrystal generated using the Wulff construction using the *MPInterfaces* code. The code excerpt used for the creation of nanoparticle is provided in the text. The PbS nanocrystal exhibits the shape of a truncated octahedron with (111) and (100) facets.

reconstruction in Figure 2. The resulting nanocrystal shape is a truncated octahedron formed by (111) and (100) facets.

---

```

# A code excerpt for generation of
# PbS nanoparticle
# All distances are in Angstroms and
# surface energies in meV per square
# Angstroms

from mpinterfaces.nanoparticle import \
    Nanoparticle

rmax = 50
hkl_family = [(1,1,1), (1,0,0), (1,1,0)]
surface_energies = [18, 24, 28]
nanoparticle = Nanoparticle(
    bulk_structure,
    rmax=rmax,
    hkl_family=hkl_family,
    surface_energies=
        surface_energies)
nanoparticle.create()

```

---

## 2.3. Heterostructure Interfaces

The first step in the study of heterojunctions of solid-state materials is the construction of the interface between two crystal structures. This construction is challenging due to the fact that there are usually numerous possible coincident site lattices (CSLs) [38, 10], which can be used to create the heterostructure interface. Moreover, additional

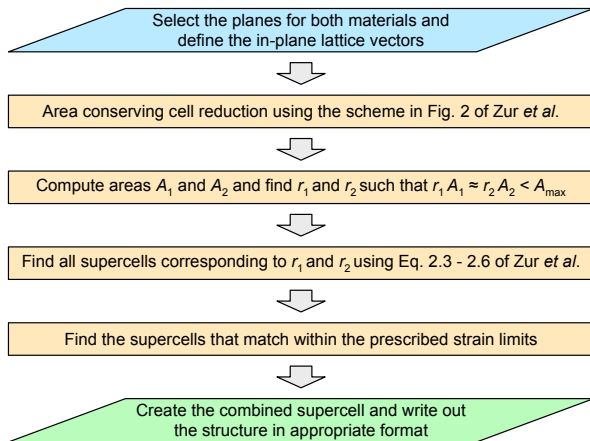


Figure 3: The algorithm of Zur *et al.* [39] for the epitaxial lattice-matching and symmetry-matching of any two surfaces for all rotations; within a given lattice mismatch and within a given surface area of the interface.

possibilities arise due to all the possible placement of atoms at the interface. A very simplistic approach would be to do a brute force search of the coincidence lattice vectors between two surfaces. However this is not only inefficient but is also inapplicable for surfaces with different crystal symmetry [10].

In the *MPInterfaces* package we implemented an algorithm, which rapidly scans through various interface configurations for an interface between two crystal surfaces and identifies those pairs that are within a specified lattice-mismatch, symmetry-matched, and distinct from each other. Figure 3 illustrates the efficient lattice matching algorithm proposed by Zur *et al.* [39], which we employ to identify the lattice and symmetry matched interfaces for any two crystal surfaces and arbitrary rotations. First, the number of possible CSLs in this algorithm depends on the maximum permitted interface area and the maximum lattice-mismatch that the interface is allowed to undergo. Second, the surface matching of the interface atoms is performed by identifying the distinct atoms in the near-interface layers and creating all distinct structures formed by placing the non-distinct atoms on top of each other.

Combined with the input file generation and workflow management features of *MPInterfaces*, this algorithm can be used to perform high-throughput computational screening of suitable substrates for 2D material deposition and function-

Table 1: Identification of the interface structure for graphene on seven possible metal (111) substrates. The lattice parameter,  $a$  (Å), of the (111) surfaces of Pt, Cu, Au, Pt, Ni, Al and Ag are shown, together with lattice-mismatch between the primitive lattices of graphene and the substrates,  $\epsilon_{1:1}$  in (%), and compared with the lattice-mismatches obtained from the *MPInterfaces* code,  $\epsilon_{MPInt}$  (%). The supercells of substrate,  $S_{sub}$ , and graphene,  $S_{gr}$ , obtained from *MPInterfaces* are provided as well.

	$a$	$\epsilon_{1:1}$	$\epsilon_{MPInt}$	$S_{sub}$	$S_{gr}$
Pt	3.98	12.55	0.98	$\sqrt{3} \times \sqrt{3}$	$2 \times 2$
Cu	3.62	3.92	-3.92	$1 \times 1$	$1 \times 1$
Au	4.17	16.45	-3.53	$\sqrt{3} \times \sqrt{3}$	$2 \times 2$
Pd	3.95	11.71	1.94	$\sqrt{3} \times \sqrt{3}$	$2 \times 2$
Ni	3.52	0.93	-0.93	$1 \times 1$	$1 \times 1$
Al	4.07	14.37	-1.12	$\sqrt{3} \times \sqrt{3}$	$2 \times 2$
Ag	4.14	15.82	-2.79	$\sqrt{3} \times \sqrt{3}$	$2 \times 2$

alization [40]. Given a list of 2D materials and substrates, using the *MPInterfaces* package we find the CSLs for each substrate/2D material pair and subsequently generate the structure files for the combined structure for further DFT or MD analysis. A study of the thermodynamics of the system and effects of substrate on the 2D material properties can reveal if the growth of a particular 2D materials is feasible on that substrate; and if the substrate alters any of the 2D materials properties [40, 41, 42, 43, 44].

As an illustrative example, we apply the *MPInterfaces* framework to determine the lattice-matches of graphene with seven potential metal substrates. Graphene has a hexagonal lattice with a lattice parameter of 2.46 Å. Table 4 lists the lattice-mismatch between graphene and the (111) surfaces of Pt, Pd, Cu, Ag, Ni, Au and Al. A 1:1 match between the primitive cells of graphene and substrate results in lattice-mismatches,  $\epsilon_{1:1}$ , exceeding 10%, except for Cu and Ni. *MPInterfaces* identifies that a  $\sqrt{3} \times \sqrt{3}$  supercell of all the other metal (111) surfaces is matched with the  $2 \times 2$  surface of graphene within a lattice mismatch,  $\epsilon_{MP} < 4\%$ . Figure 4 shows a schematic of the interfaces obtained for graphene and the seven substrates and the following code excerpt illustrates how the lattice matches are obtained in *MPInterfaces*.

```

# A code excerpt for generation of interfaces
# between graphene and substrates
# within a give lattice mismatch and maximum
# area of the interface surface
# All distances are in Angstroms and lattice
  
```

```

# mismatches in percent

from mpinterfaces.interface import Interface
from mpinterfaces.transformations import *
from mpinterfaces.utils import *

separation = 3
nlayers_2d = 2
nlayers_substrate = 2
# Lattice matching algorithm parameters
max_area = 400
max_mismatch = 4
max_angle_diff = 1
r1r2_tol = 0.01

substrate_bulk = Structure.from_file(
    'POSCAR_substrate')
substrate_slab = Interface(substrate_bulk,
    hkl = [1,1,1],
    min_thick = 10,
    min_vac = 25,
    primitive = False,
    from_ase = True)
mat2d_slab = slab_from_file([0,0,1],
    'POSCAR_2D')

# get aligned lattices
substrate_slab_aligned, mat2d_slab_aligned =
    get_aligned_lattices(
        substrate_slab,
        mat2d_slab,
        max_area = max_area,
        max_mismatch = max_mismatch,
        max_angle_diff = max_angle_diff,
        r1r2_tol = r1r2_tol)

# merge substrate and mat2d in all possible
# ways
hetero_interfaces = generate_all_configs(
    mat2d_slab_aligned,
    substrate_slab_aligned,
    nlayers_2d,
    nlayers_substrate,
    separation

```

#### 2.4. Workflows

Any computational analysis of a materials system involves an initial setup of a computational model (generation of the interface models as described in previous sections), a series of calculations which may depend on each other and optional automated post processing of the computed data to extract information and knowledge. This constitutes a computational workflow. The *MPInterfaces* package supports the writing of simple computational workflows where each step is a Python func-

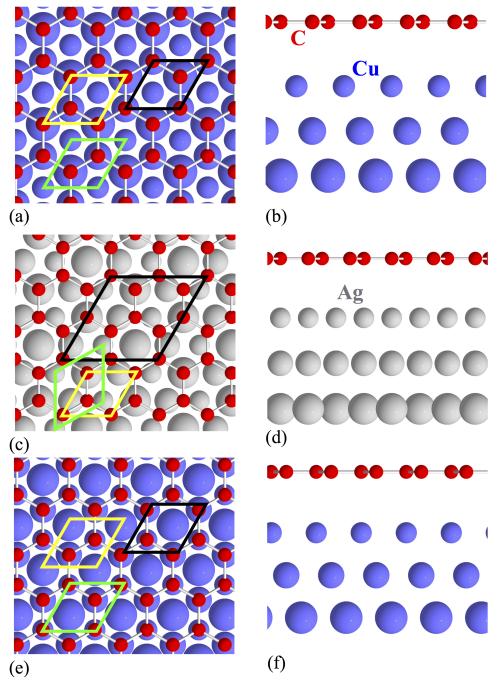


Figure 4: (a) Top view and (b) side view of 1:1 match between strained graphene and Cu(111) (or Ni(111)). (c) Top view and (d) side view of  $2 \times 2$  graphene strained by  $< 4\%$  to match the  $\sqrt{3} \times \sqrt{3}$  supercells of Ag(111) (or Pd(111), Pt(111), Au(111) and Al(111)) surfaces. The primitive cell of graphene is shown with a yellow box, that of the substrates with a green box, and lattice-matched cells of graphene and substrates with a black box. Another configuration for (a) is shown in (e) top view and (f) side view, but with a different surface placement of the atoms at the interface. The substrate atoms beyond the third layer from the interface are hidden for clarity.

tion that can take as arguments the values returned by the Python function of the preceding step.

The computational job management and workflow creation extends the Materials Project packages *Custodian* [25] and *Fireworks* [26]. In comparison to the Fireworks workflows that links together objects of the Fireworks class in a direct acyclic graph (DAG), our workflows constitute simple linearly connected jobs described by Python functions. A major difference between this workflow and that of Fireworks is that we do not use a database for the archiving and launching of workflows; this design aspect of Fireworks enables fetching of the workflows from a remote database when in need and the subsequent launching of jobs in the workflow on the cluster. We built on these workflow ideas, and developed a simple and portable workflow creation and job management system, that manages



computational high throughput discovery projects run on differing job queue systems like SLURM and PBS.

Our workflows are typically a combination of sequences of structure input and manipulation, and the calculation of the energy or a material property of the structure, and post processing of calculated data to extract required information. Each workflow is divided into steps, which can be any part of the aforementioned sequence.

Our workflow design employs simple Java serializable object notation (JSON) checkpoint files for keeping track of the jobs and their completion status on the queue. The checkpoint files provide a concise logging of the energies calculated for each calculation in a single file together with information on input files and parameters used for each calculation in the workflow.

The checkpoint feature also enables a comprehensive logging of errors and the handling of specific error measures to ensure successful completion of the workflow. This aids in the subsequent analysis of error sources and directs specific error handling corrections to the appropriate jobs, where we could not apply generalized auto-correction schemes. We find the error handling particularly useful in for queue errors, which can be as high as 10% on large supercomputing clusters. We adopted this simplified implementation to avoid the need for administrative privilege to setup up a dedicated workflow database on each individual computational resource. Our approach also simplifies the setting up of the workflow environment on arbitrary computing resources.

We note and highlight that the job management system caters to the loads of general investor queues on large supercomputer clusters like HiPerGator and the XSEDE resources of Stampede which use the PBS and SLURM job scheduling systems respectively. In addition, partition batch jobs management implemented in this high throughput materials analysis framework facilitates a controlled load on the job scheduler.

To illustrate the features of *MPInterfaces*, we describe in the following the two computational workflows that create interfaces structures, perform DFT and MD simulations, respectively, followed by the subsequent extraction of information.

#### 2.4.1. VASP workflow example

Figure 5 illustrates an example for a DFT workflow that employs the VASP code to investigate the ligand adsorption on nanocrystal facets. The

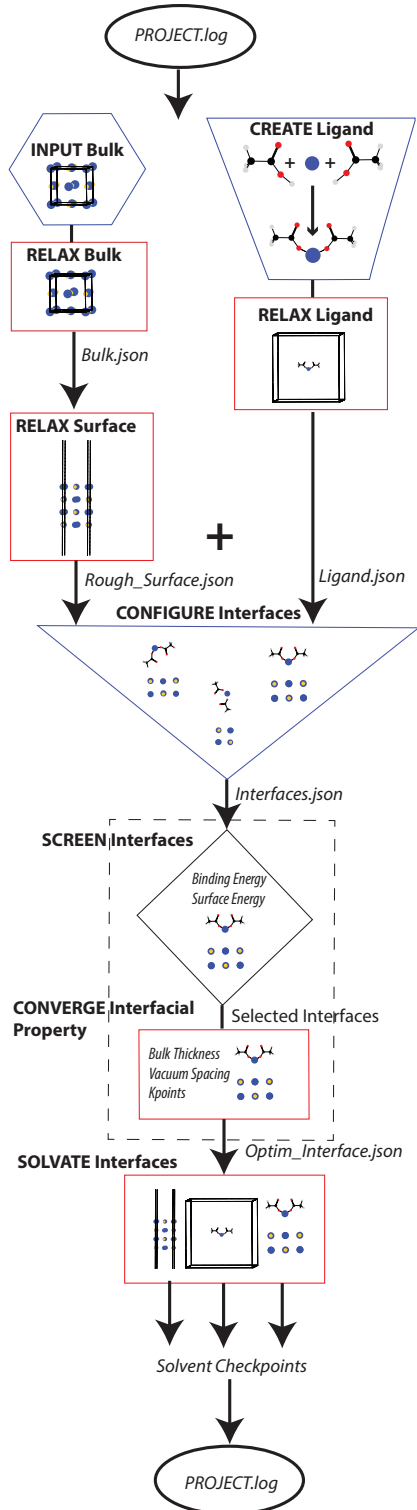


Figure 5: Workflow to study the adsorption of lead acetate ligands on PbS nanocrystal facets using DFT.

materials' system considered is the adsorption of lead acetate ligands on PbS facets.

After assembling two acetic acid molecules and a Pb atom to form the ligand, lead acetate, the first step is to relax the ligand molecule. The PbS bulk phase is relaxed and slabs are created and relaxed for the appropriate surface facets. The execution of each step results in a JSON checkpoint file that is passed on to the subsequent steps. Combining the information from the ligand and surface slab relaxation checkpoint files, the next step creates and relaxes ligand adsorption configurations with different adsorption sites, ligand orientations, ligand densities *etc.* as described in Section 2.1. The final step extracts the required interfacial properties such as surface and binding energies and optionally perform solvation calculations with VASPsol [30, 32, 33, 45] to estimate the effect of solvents or electrolytes on surface and binding energies.

#### 2.4.2. LAMMPS workflow example

*MPInterfaces* also provides an interface to the widely used MD code, LAMMPS [24]. Figure 6 illustrates the workflow for the calculation of the surface energies of Al facets with an empirical energy model implemented into LAMMPS to construct the shape of Al nanocrystals using the Wulff construction. The workflow consists of two steps. First, a geometric optimization is performed for the bulk phase of Al and the constructed low-index Al facets. The LAMMPS calculations employ the COMB3 [46] empirical potential. The second step uses the energies obtained from the first step to compute the surface energies and performs a Wulff construction implemented in the *MPInterfaces* package to create the nanocrystal shape.

### 3. Summary

We have implemented a materials project based open-source Python package, *MPInterfaces*, that extends the capabilities of existing high-throughput frameworks such as pymatgen, custodian and fireworks, towards the study of interfacial systems. The package is being continuously developed and is hosted on GitHub at <https://github.com/henniggroup/MPInterfaces>. We demonstrate the usefulness of the package and its capabilities by various illustrative examples accompanied by their corresponding code excerpts. Through the reuse of existing efficient Python tools, with this open-source

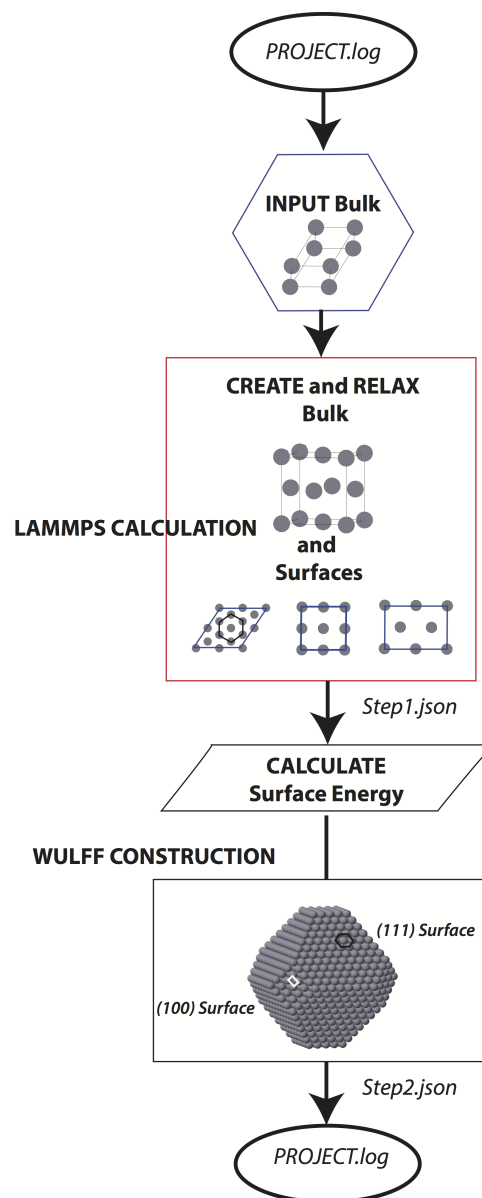


Figure 6: Workflow to predict the shape of aluminum nanocrystals using empirical energy models with the LAMMPS code.



undertaking, we intent to provide a collaborative platform that welcomes any interested user to review and improve the code base and help push the limits of state of the art computational modeling of interfaces.

#### 4. Acknowledgments

K. Mathew and R. G. Hennig are funded by the National Science Foundation under the CAREER award No. DMR-1056587 and the award No. ACI-1440547, and by the National Institute of Standards and Technology (NIST) under award 00095176. A. Singh is funded by the Professional Research Experience Postdoctoral Fellowship under award No. 70NANB11H012. J. J. Gabriel, F. Tavazza and A. Davydov are funded by the Material Genome Initiative funding allocated to NIST. This research used computational resources provided by the University of Florida Research Computing (<http://researchcomputing.ufl.edu>) and the Texas Advanced Computing Center under Contracts TG-DMR050028N, TG-DMR140143, and TG-DMR150006. This work used the Extreme Science and Engineering Discovery Environment (XSEDE), which is supported by National Science Foundation grant number ACI-1053575.

#### References

- [1] J. Joo, H. B. Na, T. Yu, J. H. Yu, Y. W. Kim, F. Wu, J. Z. Zhang, T. Hyeon, Generalized and facile synthesis of semiconducting metal sulfide nanocrystals., *Journal of the American Chemical Society* 125 (36) (2003) 11100–5. doi:10.1021/ja0357902.  
URL <http://www.ncbi.nlm.nih.gov/pubmed/12952492>
- [2] J. Park, K. An, Y. Hwang, J.-G. Park, H.-J. Noh, J.-Y. Kim, J.-H. Park, N.-M. Hwang, T. Hyeon, Ultra-large-scale syntheses of monodisperse nanocrystals., *Nature materials* 3 (12) (2004) 891–5. doi:10.1038/nmat1251.  
URL <http://www.ncbi.nlm.nih.gov/pubmed/15568032>
- [3] D. Bera, L. Qian, T.-K. Tseng, P. H. Holloway, Quantum Dots and Their Multimodal Applications: A Review, *Materials* 3 (4) (2010) 2260–2345. doi:10.3390/ma3042260.  
URL <http://www.mdpi.com/1996-1944/3/4/2260/>
- [4] D.-h. Ha, A. H. Caldwell, M. J. Ward, S. Honrao, K. Mathew, R. Hovden, M. K. a. Koker, D. a. Muller, R. G. Hennig, R. D. Robinson, Solid Solid Phase Transformations Induced through Cation Exchange and Strain in 2D Heterostructured Copper Sulfide Nanocrystals, *Nano letters*.
- [5] Y. Lu, Z. Tu, L. a. Archer, Stable lithium electrodeposition in liquid and nanoporous solid electrolytes, *Nature Materials* 13 (October) (2014) 961–969. doi:10.1038/nmat4041.  
URL <http://www.nature.com/doifinder/10.1038/nmat4041>
- [6] W. J. Baumgardner, K. Whitham, T. Hanrath, Confined-but-Connected Quantum Solids via Controlled Ligand Displacement., *Nano letters*doi:10.1021/nl401298s.  
URL <http://www.ncbi.nlm.nih.gov/pubmed/23777454>
- [7] C. R. Bealing, W. J. Baumgardner, J. J. Choi, T. Hanrath, R. G. Hennig, Predicting nanocrystal shape through consideration of surface-ligand interactions, *ACS Nano* 6 (3) (2012) 2118–2127. doi:10.1021/nn3000466.
- [8] G. Ceder, Y.-M. Chiang, D. R. Sadoway, M. K. Aydinol, Y.-I. Jang, B. Huang, Identification of cathode materials for lithium batteries guided by first-principles calculations, *Nature* 392 (April) (1998) 694–696. doi:10.1038/33647.  
URL <http://dx.doi.org/10.1038/33647>
- [9] J. J. Choi, C. R. Bealing, K. Bian, K. J. Hughes, W. Zhang, D.-M. Smilgies, R. G. Hennig, J. R. Engstrom, T. Hanrath, Controlling nanocrystal superlattice symmetry and shape-anisotropic interactions through variable ligand surface coverage., *Journal of the American Chemical Society* 133 (9) (2011) 3131–8. doi:10.1021/ja110454b.  
URL <http://www.ncbi.nlm.nih.gov/pubmed/21306161>
- [10] J. Hwang, D. Campbell, S. Shivaraman, H. Alsalman, J. Y. Kwak, M. Kim, A. R. Woll, A. K. Singh, R. G. Hennig, S. Gorantla, M. H. Rummeli, M. G. Spencer, Van der waals epitaxial growth of graphene on sapphire by CVD without a metal catalyst, *ACS Nano* 7 (2013) 385.
- [11] D.-H. Ha, L. M. Moreau, S. Honrao, R. G. Hennig, R. D. Robinson, The oxidation of cobalt nanoparticles into kirkendall-hollowed  $\text{CoO}$  and  $\text{Co}_3\text{O}_4$ : the diffusion mechanisms and atomic structural transformations, *The Journal of Physical Chemistry C* 117 (27) (2013) 14303–14312.
- [12] B. Anasori, Y. Xie, M. Beidaghi, J. Lu, B. C. Hosler, L. Hultman, P. R. C. Kent, Y. Gogotsi, M. W. Barsoum, Two-Dimensional, Ordered, Double Transition Metals Carbides (MXenes)., *ACS nano* (2015) 9507–9516doi:10.1021/acsnano.5b03591.  
URL <http://dx.doi.org/10.1021/acsnano.5b03591>
- [13] R. B. van Dover, L. Schneemeyer, R. Fleming, Discovery of a useful thin-film dielectric using a composition-spread approach, *Nature* 392 (6672) (1998) 162–164.
- [14] H. Koinuma, I. Takeuchi, Combinatorial solid-state chemistry of inorganic materials, *Nature materials* 3 (7) (2004) 429–438.
- [15] I. Takeuchi, J. Lauterbach, M. J. Fasolka, Combinatorial materials synthesis, *Materials Today* 8 (10) (2005) 18 – 26. doi:http://dx.doi.org/10.1016/S1369-7021(05)71121-4.  
URL <http://www.sciencedirect.com/science/article/pii/S1369702105711214>
- [16] A. K. Singh, K. Mathew, H. L. Zhuang, R. G. Hennig, Computational screening of 2D materials for photocatalysis, *The Journal of Physical Chemistry Letters* 6 (6) (2015) 1087–1098.
- [17] L. Cheng, R. S. Assary, X. Qu, A. Jain, S. P. Ong, N. N. Rajput, K. Persson, L. A. Curtiss, Accelerating electrolyte discovery for energy storage with high-throughput screening, *The Journal of Physical Chemistry Letters* 6 (2) (2015) 283–291. doi:10.1021/

- jz502319n.
- [18] R. Armiento, B. Kozinsky, M. Fornari, G. Ceder, Screening for high-performance piezoelectrics using high-throughput density functional theory, *Phys. Rev. B* 84 (2011) 014103. doi:10.1103/PhysRevB.84.014103. URL <http://link.aps.org/doi/10.1103/PhysRevB.84.014103>
- [19] J. Greeley, J. K. Nørskov, Combinatorial density functional theory-based screening of surface alloys for the oxygen reduction reaction, *The Journal of Physical Chemistry C* 113 (12) (2009) 4932–4939. doi:10.1021/jp808945y.
- [20] M. P. Andersson, T. Bligaard, A. Kustov, K. E. Larsen, J. Greeley, T. Johannessen, C. H. Christensen, J. K. Nørskov, Toward computational screening in heterogeneous catalysis: Pareto-optimal methanation catalysts, *Journal of Catalysis* 239 (2) (2006) 501–506.
- [21] J. Greeley, T. F. Jaramillo, J. Bonde, I. Chorkendorff, J. K. Nørskov, Computational high-throughput screening of electrocatalytic materials for hydrogen evolution, *Nature materials* 5 (11) (2006) 909–913.
- [22] J. Greeley, I. E. L. Stephens, a. S. Bondarenko, T. P. Johansson, H. a. Hansen, T. F. Jaramillo, J. Rossmeisl, I. Chorkendorff, J. K. Nørskov, Alloys of platinum and early transition metals as oxygen reduction electrocatalysts., *Nature chemistry* 1 (7) (2009) 552–556. doi:10.1038/nchem.367. URL <http://dx.doi.org/10.1038/nchem.367>
- [23] G. Kresse, J. Furthmüller, *Comput. Mater. Sci.* 6 (1996) 15–50.
- [24] S. Plimpton, Fast Parallel Algorithms for Short Range Molecular Dynamics, *Journal of Computational Physics* 117 (June 1994) (1995) 1–19. doi:10.1006/jcph.1995.1039.
- [25] S. P. Ong, W. D. Richards, A. Jain, G. Hautier, M. Kocher, S. Cholia, D. Gunter, V. L. Chevrier, K. A. Persson, G. Ceder, Python Materials Genomics (pymatgen): A robust, open-source python library for materials analysis, *Computational Materials Science* 68 (2013) 314–319. doi:10.1016/j.commatsci.2012.10.028. URL <http://linkinghub.elsevier.com/retrieve/pii/S0927025612006295>
- [26] A. Jain, S. P. Ong, W. Chen, B. Medasani, X. Qu, M. Kocher, M. Brafman, G. Petretto, G.-M. Rignanese, G. Hautier, D. Gunter, K. A. Persson, Fireworks: a dynamic workflow system designed for high-throughput applications, *Concurrency and Computation: Practice and Experience* doi:10.1002/cpe.3505. URL <http://dx.doi.org/10.1002/cpe.3505>
- [27] S. R. Bahn, K. W. Jacobsen, An object-oriented scripting interface to a legacy electronic structure code, *Comput. Sci. Eng.* 4 (3) (2002) 56–66. doi:10.1109/5992.998641.
- [28] P. Dey, J. Paul, J. Bylisma, D. Karaiskaj, J. Luther, M. Beard, a.H. Romero, Origin of the temperature dependence of the band gap of PbS and PbSe quantum dots, *Solid State Communications* 165 (2013) 49–54. doi:10.1016/j.ssc.2013.04.022. URL <http://linkinghub.elsevier.com/retrieve/pii/S0038109813001968>
- [29] W. S. E. Bohn, The renaissance of dye-sensitized solar cells, *Nature Photonics* 6 (3) (2012) 162–169. doi:10.1038/nphoton.2012.22. URL <http://www.nature.com/doi/10.1038/nphoton.2012.22>
- [30] M. Fishman, H. L. Zhuang, K. Mathew, W. Dirschka, R. G. Hennig, Accuracy of exchange-correlation functionals and effect of solvation on the surface energy of copper, *Phys. Rev. B* 87 (2013) 245402. doi:10.1103/PhysRevB.87.245402. URL <http://link.aps.org/doi/10.1103/PhysRevB.87.245402>
- [31] N. O’Boyle, M. Banck, C. James, C. Morley, T. Vandermeersch, G. Hutchison, Open babel: An open chemical toolbox, *Journal of Cheminformatics* 3 (1) (2011) 33. doi:10.1186/1758-2946-3-33.
- [32] K. Mathew, R. Sundararaman, K. Letchworth-Weaver, T. A. Arias, R. G. Hennig, Implicit solvation model for density-functional study of nanocrystal surfaces and reaction pathways, *The Journal of Chemical Physics* 140 (8) (2014) 084106.
- [33] K. Mathew, R. G. Hennig, Implicit self-consistent description of electrolyte in plane-wave density-functional theory, arXiv preprint arXiv:1601.03346.
- [34] G. Wulff, Xxv. zur frage der geschwindigkeit des wachstums und der auflösung der krystallflä, *Zeitschrift für Kristallographie* 34 (1901) 449–530. doi:10.1524/zkri.1901.34.1.449.
- [35] I. Fonseca, The wulff theorem revisited, *Proceedings of the Royal Society of London A: Mathematical, Physical and Engineering Sciences* 432 (1884) (1991) 125–145. arXiv:<http://rspa.royalsocietypublishing.org/content/432/1884/125.full.pdf>, doi:10.1098/rspa.1991.0009. URL <http://rspa.royalsocietypublishing.org/content/432/1884/125>
- [36] K. C. Kim, B. Dai, J. Karl Johnson, D. S. Sholl, Assessing nanoparticle size effects on metal hydride thermodynamics using the Wulff construction., *Nanotechnology* 20 (20) (2009) 204001. doi:10.1088/0957-4484/20/20/204001. URL <http://www.ncbi.nlm.nih.gov/pubmed/19420649>
- [37] J. Heyraud, J. Métois, Equilibrium shape and temperature; Lead on graphite, *Surface Science* 128 (1983) 334–342. doi:10.1016/S0039-6028(83)80036-3.
- [38] A. Santoro, A. D. Mighell, Coincidence-site lattices, *Acta Crystallographica Section A* 29 (2) (1973) 169–175. doi:10.1107/S0567739473000434.
- [39] A. Zur, T. McGill, Lattice match: An application to heteroepitaxy, *Journal of Applied Physics* 55 (2) (1984) 378–386.
- [40] A. K. Singh, K. Mathew, A. V. Davydov, R. G. Hennig, F. Tavazza, High throughput screening of substrates for synthesis and functionalization of 2D materials, *Proc. SPIE* 9553 (2015) 955316–955316–8. doi:10.1117/12.2192866.
- [41] A. K. Singh, R. G. Hennig, A. V. Davydov, F. Tavazza, Al<sub>2</sub>O<sub>3</sub> as a suitable substrate and a dielectric layer for *n*-layer MoS<sub>2</sub>, *Applied Physics Letters* 107 (5) (2015) 053106.
- [42] A. K. Singh, H. L. Zhuang, R. G. Hennig, Ab initio synthesis of single-layer III-V materials, *Physical Review B* 89 (2014) 245431. doi:10.1103/PhysRevB.89.245431. URL <http://link.aps.org/doi/10.1103/PhysRevB.89.245431>
- [43] A. K. Singh, R. G. Hennig, Computational synthesis of single-layer GaN on refractory materials, *Applied Physics Letters* 105 (5) (2014) 051604.
- [44] H. L. Zhuang, A. K. Singh, R. G. Hennig, Computational discovery of single-layer III-V materials, *Physical*

Review B 87 (16) (2013) 165415.

- [45] K. Mathew, R. G. Hennig, VASPsol - Solvation model for the plane wave DFT code VASP, <https://github.com/henniggroup/VASPsol> (2015).
- [46] K. Choudhary, T. Liang, A. Chernatynskiy, S. R. Phillpot, S. B. Sinnott, Charge optimized many-body (comb) potential for  $\text{Al}_2\text{O}_3$  materials, interfaces, and nanostructures, *Journal of Physics: Condensed Matter* 27 (30) (2015) 305004.